

Spatial Filter Approach for Comparison of the Forward and Inverse Problems of Electroencephalography and Magnetoencephalography

L. A. BRADSHAW,^{1,3} R. S. WIJESINGHE,² and J. P. WIKSWO, JR.¹

¹Living State Physics Group, Department of Physics and Astronomy, Vanderbilt University, Nashville, TN,

²Brain Physics Group, Department of Biomedical Engineering, Tulane University, New Orleans, LA,

and ³Department of Physics and Engineering Science, Lipscomb University, Nashville, TN

(Received 11 January 2000; accepted 5 January 2001)

Abstract—We present an analysis of the relative information content of cortical current source reconstructions from electroencephalogram (EEG) and magnetoencephalogram (MEG) forward calculations by examining the spatial filters that relate the internal sources with the externally measured electric potentials and magnetic fields. The forward spatial filters are seen to be low-pass functions of spatial frequency and spatial resolution degrades in external measurements. Inverse spatial filters may be used to reconstruct cortical sources from external data, but since they are high-pass functions of spatial frequency, they must be regularized to avoid instabilities caused by noise at higher spatial frequencies. The regularization process limits the spatial resolution of source reconstructions. EEG forward spatial filters fall off at lower spatial frequencies than MEG filters; hence, there is less information available in higher spatial frequencies resulting in lower spatial resolution in inverse reconstructions. The tangential component of the magnetic field provides even higher spatial resolution than can be obtained using the radial component. An accompanying article examines the surface Laplacian for both the EEG and the MEG. © 2001 Biomedical Engineering Society. [DOI: 10.1114/1.1352641]

Keywords—Magnetoencephalogram, Electroencephalogram, Inverse problem, Spatial resolution, Biomagnetism.

INTRODUCTION

The question of the relative information content in electroencephalogram (EEG) and magnetoencephalogram (MEG) signals has interested many researchers.⁵² The fundamental advantage of both the EEG and the MEG over other functional imaging modalities that measure blood flow changes and other vascular phenomena such as positron emission tomography, single-photon emission computed tomography, and magnetic resonance imaging (MRI) is the increased temporal resolution—milliseconds versus seconds to minutes for these competing techniques.⁴⁶ Functional MRI images may be obtained in 50 ms, but the longer time constant for blood diffusion

further restricts the temporal resolution. In contrast, the EEG and MEG measure brain electrical activity directly.

SPATIAL RESOLUTION

The question of the relative information contained in the MEG versus that of the EEG is one that must be answered if the additional cost of the MEG is to be justified, and thus has been a subject of recent debate. One of the most important issues is that of spatial resolution, or the accuracy with which cortical sources of the EEG and MEG signals may be reconstructed. The debate is confined to the case of superficial cortical sources that are not oriented perpendicular to the head surface since it is well established that the EEG is more sensitive to deep cortical sources and to radial sources than the MEG. Although numerous theoretical studies had shown that the MEG could potentially boast an order of magnitude improvement in spatial localizing power,^{12,13} a study using dipoles implanted in human patients claimed that the MEG provided relatively little improvement to the localization of dipoles.¹¹ Although that study was widely criticized on the basis of outdated methodology,^{23,54} and the majority of the literature supports the view that the localizing power of the MEG is significantly greater than that of the EEG,^{4,33,34} a few authors have since presented theoretical arguments that the spatial resolution of the MEG is comparable to that of the EEG.^{32,38}

This article contributes to the EEG/MEG debate by representing the relationships between cortical current sources and external magnetic fields and electric potentials as filters in the spatial frequency domain which are easily visualized as Fourier transforms. Thus, the spatial filter formulation explicitly characterizes the effect of the geometry and conductivity profile of the volume conductor model. Since the external fields and potentials are typically noisy, they are unstable upon inversion and must be regularized. The spatial filter framework also allows quantification of the degree of regularization necessary to achieve stable inverse solutions from noisy

Address correspondence to Alan Bradshaw, PhD, Dept. of Physics, Box 1807, Station B, Vanderbilt University, Nashville, TN 37235. Electronic mail: alan.bradshaw@vanderbilt.edu

measured data, and shows the effect of regularization on inverse stability and spatial resolution. Using the spatial filters for the EEG and MEG to evaluate their spatial resolution in a simple model will thus provide basic insights into the fundamental similarities and differences between electric and magnetic forward and inverse problems. For these reasons, spatial filters are a convenient basis for discussions of EEG/MEG spatial resolution.

The concept of spatial resolution is somewhat ambiguous since it is often used to refer to either the accuracy with which a particular source is localized (localizing resolution) or the ability to distinguish the presence of multiple sources (imaging resolution). These two separate concepts of localizing resolution and imaging resolution are independent measures of spatial resolution.^{31,42,51} For inverse procedures that model current sources as single dipoles, imaging resolution and localizing resolution are synonymous since dipoles are defined at a single location and have no spatial extent.⁹ Multiple-dipole and distributed source solutions, however, may have different imaging and localizing resolution, since both the location and size of the active region are estimated.²¹ Wiksw⁵¹ estimates that localizing resolution for MEG may be on the order of a few millimeters, whereas imaging resolution is an order of magnitude larger, several centimeters. While we will not attempt to establish fundamental numerical limits on EEG or MEG spatial resolution, we can use the concept of spatial filters to investigate the spatial resolution of inverse reconstructions from EEG and MEG data.

SPATIAL FILTERS

The volume conducting properties of the head alter the external magnetic field and the scalp electric potential.^{10,17,18} The low conductivity of the skull tends to reduce the electric potential. Both the potential and magnetic field are also affected by the skull geometry. Tan *et al.*,⁴⁹ and several other authors^{14,27,30,43,47,50,53,56} have used a spatial filter approach to model external fields or potentials as modified, or filtered, versions of the internal sources. These researchers found that forward spatial filters that describes the external measured fields and potentials in terms of the internal sources are low-pass functions of spatial frequency. In other words, external fields and potentials are smoothed and attenuated versions of the internal sources. Thus, some degree of spatial information about the source is absent from the externally measured fields and potentials.

The analysis of Tan *et al.*⁴⁹ describe the external magnetic field $\mathbf{B}(\mathbf{r})$ in terms of the internal current source density $\mathbf{J}(\mathbf{r})$ by means of the spatial filter

$$\mathbf{b}(r, \theta, k_z) = g^{jb}(r, \theta, k_z) \mathbf{j}(r, \theta, k_z), \quad (1)$$

where lower-case characters indicate the one-dimensional Fourier transforms of the corresponding upper-case quantities. We may represent the electric potential $\Phi(\mathbf{r})$ similarly as

$$\phi(r, \theta, k_z) = g^{j\phi}(r, \theta, k_z) \mathbf{j}(r, \theta, k_z). \quad (2)$$

Equations (1) and (2) express the source-measurement relationship in the spatial frequency (k_z) domain. The functions $g^{j\phi}(r, \theta, k_z)$ and $g^{jb}(r, \theta, k_z)$ are generally low-pass functions of spatial frequency and are called forward spatial filter functions since they act on the source functions $\mathbf{j}(r, \theta, k_z)$ to produce the forward fields [Figs. 1(a)–1(e)].

The inverse problem is to determine information about the sources from externally measured data, i.e., to estimate $\mathbf{J}(\mathbf{r})$ from measurements of $\Phi(\mathbf{r})$ or $\mathbf{B}(\mathbf{r})$. Although it is normally quite difficult to obtain closed-form solutions for inverse problems in spatial coordinates, the spatial filter construct applied to a cylindrical model allows the inverse problem to be expressed simply in the spatial frequency domain. The source current density is reconstructed from the measured data by simply multiplying Eqs. (1) and (2) by the reciprocals of the forward spatial filters

$$\mathbf{j}^b(r, \theta, k_z) = \frac{1}{g^{jb}(r, \theta, k_z)} \mathbf{b}(r, \theta, k_z), \quad (3)$$

$$\mathbf{j}^\phi(r, \theta, k_z) = \frac{1}{g^{j\phi}(r, \theta, k_z)} \phi(r, \theta, k_z). \quad (4)$$

We can define new functions

$$g^{bj}(r, \theta, k_z) = \frac{1}{g^{jb}(r, \theta, k_z)}, \quad (5)$$

$$g^{\phi j}(r, \theta, k_z) = \frac{1}{g^{j\phi}(r, \theta, k_z)}, \quad (6)$$

that represent the inverse spatial filter functions. These inverse filters describe the relationship between the externally observed fields and reconstructed current density sources and are generally high pass in nature since they are reciprocals of the forward spatial filters.

Measurement noise present in the externally recorded fields and potentials, as well as physiological noise from brain sources, may distort the inverse reconstruction; the high-pass inverse filters amplify noise. The inverse problem is thus unstable and must be regularized. Regularization of inverse filters is accomplished in a straightfor-

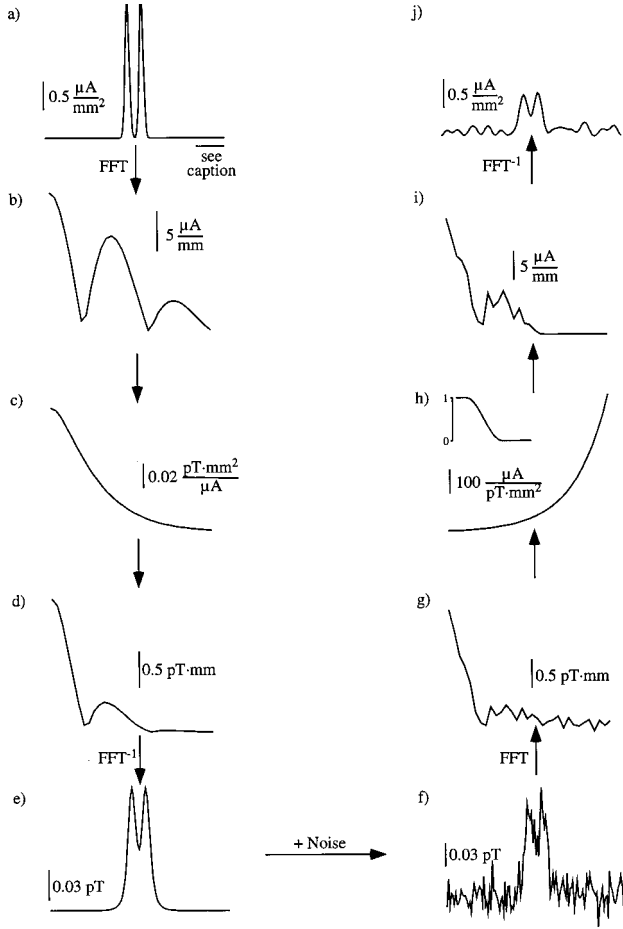


FIGURE 1. Forward and inverse calculations. The internal current density (a) is Fourier transformed (b) and multiplied by the forward spatial filter relating the current density to the radial magnetic field at the scalp surface (c). The product (d) is inverse transformed to obtain the external radial magnetic field calculated at the scalp surface (e). To simulate a measurement, noise is added to the external field (f) and the signal is again Fourier transformed (g). The transform is multiplied with the inverse spatial filter (h) and windowed to regularize the inversion using a Tukey window [inset in (h)]. The product (i) is inverse transformed to yield the source current density (i) that has been reconstructed from noisy external magnetic field data. The scale bars in (a) apply to all panels. The calibration for the horizontal bar is 2 cm for the z axis in the spatial domain in panels (a), (e), (f), and (j), and 0.016 mm^{-1} for the k axis in the spatial frequency domain for panels (b), (c), (d), (g), (h), and (i).

ward manner using windows in the spatial frequency domain. We use the Tukey window³⁹

$$w(k_z; k_{\max}) = \begin{cases} \frac{1 + \cos \frac{k}{k_{\max}} \pi}{2} & k < k_{\max}, \\ 0 & k > k_{\max} \end{cases} \quad (7)$$

so that our inverse reconstructions, Eqs. (3) and (4), become

$$\mathbf{j}_{\text{windowed}}^b(r, \theta, k_z) = w(k_z; k_{\max}) g^{bj}(r, \theta, k_z) b(r, \theta, k_z), \quad (8)$$

$$\mathbf{j}_{\text{windowed}}^\phi(r, \theta, k_z) = w(k_z; k_{\max}) g^{\phi j}(r, \theta, k_z) \phi(r, \theta, k_z). \quad (9)$$

These concepts are illustrated in Figs. 1(f)–1(j).

In addition to inverse reconstructions, there is some interest in continuation of the measured fields and potentials inward toward the brain sources.^{29,49} Inward continuation is accomplished by simply using a combination of two spatial filters.⁴⁹ For instance, the potential at $r = r_1$ is related to the potential at $r = r_2$ by

$$\phi_1(r_1, \theta, k_z) = \frac{g^j \phi(r_1, \theta, k_z)}{g^j \phi(r_2, \theta, k_z)} \phi_2(r_2, \theta, k_z). \quad (10)$$

As with inverse filters, the inward continuation process is a high-pass operation in the spatial frequency domain and is subject to regularization.

Head Model

This spatial filtering construct is useful for a model study of the EEG and MEG since issues of source localization and imaging resolution in inverse procedures can be addressed graphically by examining the spatial filters under different conditions. Typically, volume conductor models of the head are spherical in shape. The previous analyses of Roth and Wiksw⁴³ and Tan *et al.*⁴⁹ used a multilayer cylindrical model for the head. The multilayer cylindrical model has the distinct advantage of mathematical tractability since the basis functions obtained by direct solution of Laplace's equation are Fourier transforms of a series of Bessel functions that can be expressed analytically in the spatial frequency domain.^{24,50} For this reason, we modeled the cortex as an infinite cylinder encased by two cylindrical layers representing skull and scalp (Fig. 2). Clearly, this model will not represent the actual geometry of the brain any more accurately than spherical or infinite half-space models, but as with those commonly accepted models, the fundamental insights into the source–measurement relationships outweigh inaccuracies from geometrical considerations. Srinivasan *et al.*⁴⁷ presented a spatial filtering analysis of the EEG with a spherical head model using spherical harmonics as basis functions, and obtained spatial filters similar to ours. Differences from spherical geometries might be more pronounced in tangential magnetic fields, which may be more influenced by geometrical considerations than radial fields.

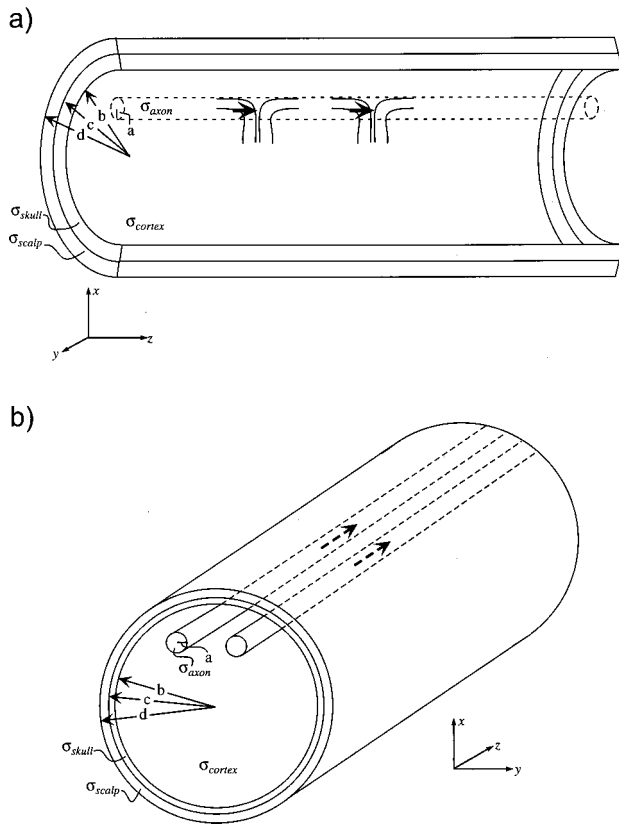


FIGURE 2. Cylindrical model of the head. The inner cylinder represents the cortex and is covered by two cylindrical layers representing skull and scalp. The conductivity ratio of cortex:skull:scalp is 80:1:80. Model parameters are listed in Table 1. Current sources are contained in an eccentric cylinder of radius a representing the effective dendrite. Two source configurations are studied: (a) two sources are aligned along the z axis; and (b) two sources are parallel to each other at the same radius and separated by a polar angle θ of 28° .

Several assumptions about model parameters are necessary. The radii of the cylinders are chosen to be consistent with earlier spherical models, as are the conductivity parameters.^{1,44} The parameter values used for this model are listed in Table 1.^{15,19} Of course, the results obtained will depend on the model parameters used here,

TABLE 1. Model parameter values.

Parameter	Value	Parameter	Value
a	0.5 mm^a	σ_{axon}	$0.88/\Omega \text{ m}^b$
b	8.0 cm^c	σ_{cortex}	$0.45/\Omega \text{ m}$
c	8.5 cm	σ_{skull}	$0.0058/\Omega \text{ m}$
d	9.2 cm	σ_{scalp}	$0.45/\Omega \text{ m}$
$ r' $	7.2 cm		

^aFrom Ref. 15.

^bFrom Ref. 19.

^cParameters b , c , d , σ_{cortex} , σ_{skull} , and σ_{scalp} are from Ref. 44.

so we will include a brief sensitivity analysis of these parameters in the Discussion.

Current Source Model

The EEG and MEG are primarily produced by the flow of current in cortical dendrites.³⁷ Source models for the EEG and MEG typically represent the summed activity of a number of these dendrites by an effective dendritic source in the manner of Rall.⁴⁰ The “effective dendrite” in this work is contained in an infinitely long cylinder of radius a situated off center at $r=t$ in the larger cylinder representing the cortex. The radius of the effective dendrite is chosen to give a cross-sectional area of roughly $10 \mu\text{m}^2$ for each of the 10^5 dendrites represented ($a=0.5 \text{ mm}$), and the conductivity is set at $0.88/\Omega \text{ m}$.^{37,48} The current source in this model is thus the intracellular current density in the effective axon that results from graded membrane potentials.⁵³ The 2 mm spatial extent of the effective dendrite is modeled by a Gaussian wave form along the z direction describing the source current density, specified by its amplitude, width, and location. Each of these parameters can be evaluated on inversion to assess spatial resolution. The amplitude of the Gaussian wave form is set at $2.5 \mu\text{A}/\text{mm}^2$, since each dendrite in the effective source has a dipole strength of about $5 \times 10^{-5} \text{ nA m}$. The z width of the Gaussian current density is set at 2 mm as suggested earlier. To address issues of spatial resolution, we use two such sources in two different configurations, as shown in Fig. 2. First, we arrange the sources in an “aligned” configuration by separating them along the longitudinal axis of the cylinder, initially separated by 1 cm, illustrated in Fig. 2(a). The second configuration is a “parallel” arrangement where two source cylinders are separated in the angular direction, initially by 28° [Fig. 2(b)]. The effect of varying the separation between sources is also considered. Radially oriented sources produce no external magnetic field, so only tangential sources are included in this analysis. Other work indicates that inclusion of nontangential orientations would degrade the performance of the MEG and enhance that of the EEG.³⁸ In the aligned case, the sources are aligned along their electric orientation, and in the parallel case, they are aligned parallel to their electric orientation.

Forward and Inverse Solutions

We use the spatial filter analysis to compare the EEG with both the radial MEG (the component normal to the calculation surface) and the tangential MEG (the component perpendicular to the cylindrical axis and tangential to the calculation surface). The magnetic fields and electric potentials are sampled along the z axis at 128 points separated by 1 mm increments for the aligned sources, and along the θ axis at 141 points separated by $\pi/128$

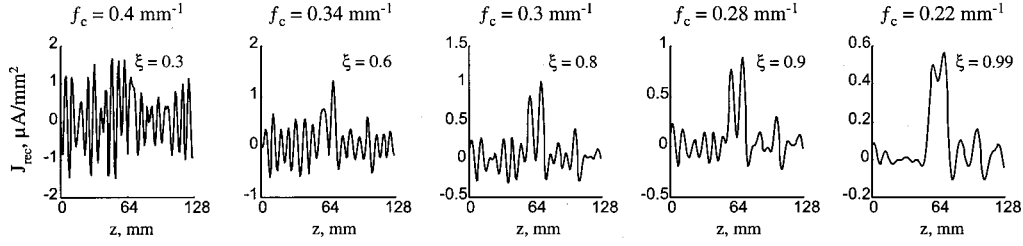


FIGURE 3. Effect of stabilizing the inversion on spatial resolution. Lower values of window cutoff frequency result in lower noise in the inversion (greater stability), but also lower spatial resolution.

rad (1.4°) increments for the parallel sources. Since the radial MEG is zero directly above the source, it was calculated at the angle at which its amplitude was maximal ($\theta = 11.5^\circ$).

In the initial calculation, random numbers simulating white measurement noise were added to the forward fields and potentials. We later consider the effect of physiological brain noise, present in the source waveform, that is concentrated at lower spatial frequencies since it is subject to the same low-pass spatial filtering as the forward solutions. A level of 30% random noise was added to the MEG signals and a level of 20% was used for the EEG. The regularized inverse filters are applied to the noisy forward signals to obtain the reconstructions, as shown in Fig. 1.

The stability of the inversion depends on two factors: the amount of noise present in the forward fields which is amplified by the inversion, and the amount of regularization applied to the inverse problem, i.e., the severity of the windowing. We define the stability of an inverse reconstruction as the ratio of the standard deviation of the reconstruction without noise in the forward signals to the standard deviation of the reconstruction from the noisy fields and potentials and represent it by ξ :

$$\xi = \frac{\sigma_{J_{\text{rec,noiseless}}|f_c}}{\sigma_{J_{\text{rec,noisy}}|f_c}}, \quad (11)$$

where σ represents the standard deviations of the noiseless and noisy reconstructed current densities. The standard deviations are evaluated at the same window cutoff frequency, f_c , i.e., for the same amount of regularization. The stability varies from a value of 0, which indicates that the noisy reconstruction has infinitely more variance than the noiseless reconstruction and so the reconstruction is perfectly unstable, to a value of 1, which indicates that the variances of the noisy and noiseless reconstructions at the same cutoff frequency are identical, and the noisy reconstruction is perfectly stable. The stability defined in this way is similar to the correlation coefficient between the noiseless and noisy inverse

reconstructions, but is more explicitly related to the signal-to-noise ratio (SNR)

$$\xi = \frac{\sigma_{J_{\text{rec,noiseless}}}}{\sigma_{J_{\text{rec,noisy}}}} = \frac{\sigma_{J_{\text{rec,noiseless}}}}{\sqrt{\sigma_{J_{\text{rec,noiseless}}}^2 + \sigma_{\text{noise}}^2}} = \frac{1}{\sqrt{1 + \frac{1}{\text{SNR}}}}. \quad (12)$$

We can use ξ to examine the trade off between stability and spatial resolution. In Fig. 3, we note that a particular inverse solution with a low stability value ($\xi = 0.3$) contains significant high spatial frequency information ($f_c = 0.4 \text{ mm}^{-1}$) but suffers from a great deal of noise. By decreasing the cutoff frequency to 0.22 mm^{-1} , the stability increases to $\xi = 0.99$ and less noise is present, but the two sources are clearly less distinct spatially. Reconstructions using intermediate values of stability and cutoff frequency are also shown. As we present inverse solutions, we shall require that the solutions obtain a stability of at least 0.96, thus allowing for a fair comparison of the two modalities of EEG and MEG.

Localizing and Imaging Resolution

We apply this approach to evaluate both the localizing and imaging resolution of the EEG and MEG. We determine the localizing resolution of the two distinct sources used here by examining the location of the two Gaussian peaks in the reconstructed current density. The imaging resolution is a measure of the distinctness of the two sources, and is related to the Gaussian widths of the two sources. In this regard, the rather conservative Rayleigh criterion used in optics to distinguish two peaks is useful. The Rayleigh criterion states that two sources are resolved if the minimum of the valley between the two peaks is less than 0.81 times the maximum of the two peaks.⁵ Tan *et al.*⁴⁹ also used this criterion to evaluate biomagnetic imaging resolution.

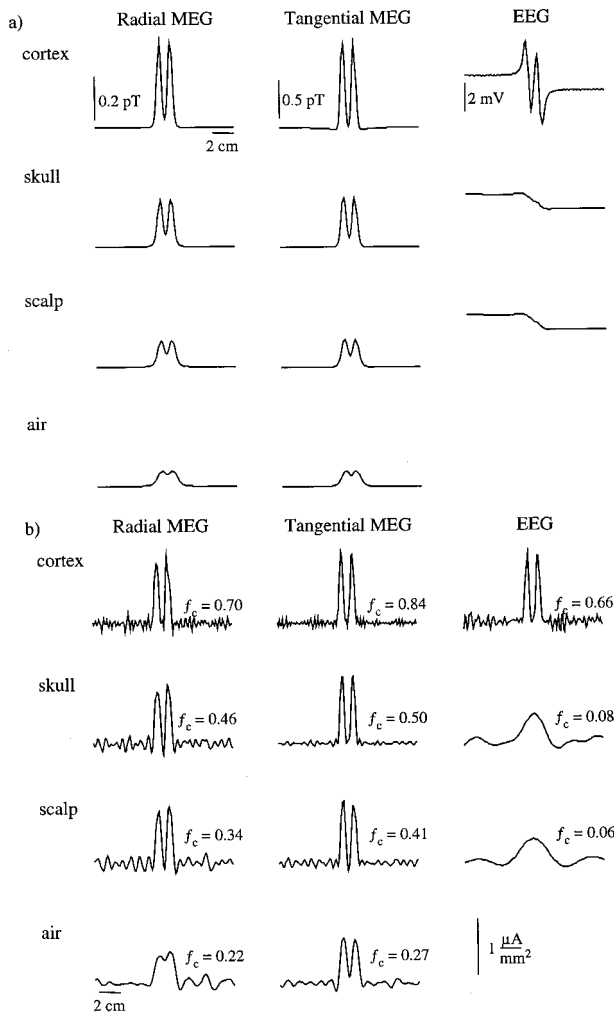


FIGURE 4. (a) Magnetic fields and potentials calculated at the surfaces of the cylindrical layers of the cortex, skull, and scalp, and the magnetic fields calculated in air 1 cm from the scalp surface. (b) Inverse reconstructions with stability >0.96 from the calculated fields shown in (a) for a source that is 2 cm beneath the scalp.

RESULTS

Volume Conductor Effects

Source Reconstructions. The potential and magnetic field from the aligned sources are shown in Fig. 4(a) at the surface of each model layer and for the MEGs in air. Sources reconstructed from these forward fields and potentials with noise added were constrained to be stable by using Tukey windows with cutoff frequencies chosen under the requirement that the stability parameter be greater than or equal to 0.96. The reconstructions are shown in Fig. 4(b) with the window cutoff frequencies indicated. These data illustrate the effects of measurement distance from the source, conductivity of intervening layers, and the relative amount of regularization necessary to keep the inverse reconstructions stable.

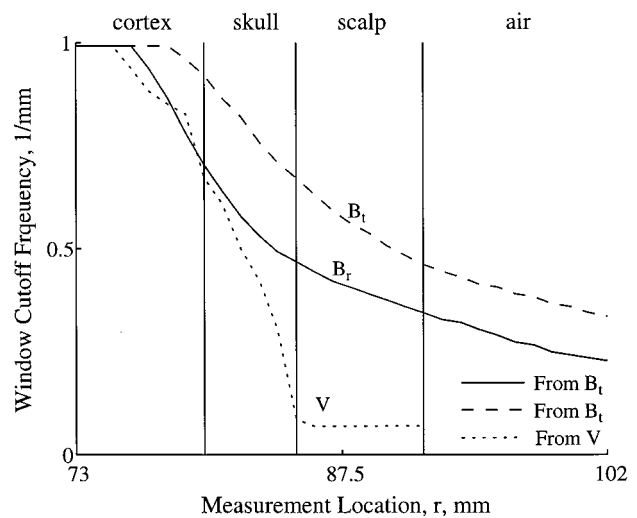


FIGURE 5. Window cutoff frequency required to produce a reconstruction with a stability of at least 0.96 as a function of measurement location. The window cutoff frequency is a measure of the degree of regularization applied to the inversion, as a low window cutoff frequency implies a high degree of regularization, and vice versa. EEG must be tremendously regularized, while inversions from MEG signals do not require as much regularization. The tangential MEG requires the least regularization and results in the highest spatial resolution.

Inverse Stability and Regularization. Figure 4(b) shows source reconstructions under the requirement that the stability be at least 0.96. More regularization is required to maintain a given stability and reject noise in the inverse solution for more superficial measurement locations. If the regularization cutoff is set at a low spatial frequency, the inverse solution will have a higher stability, but as higher frequencies are allowed in the reconstruction to increase the spatial resolution, the solutions are less and less stable. The effect of the skull is quite pronounced on the EEG signals, and a great deal of regularization (very low cutoff spatial frequency) is required to maintain stability. We can quantify these concepts further by plotting the window cutoff frequency (amount of regularization) required to maintain a stability greater than or equal to 0.96 when reconstructing sources from fields and potentials as a function of distance from the source (Fig. 5). The skull layer has a tremendous adverse effect on the reconstructions from the EEG. Outside the skull layer, only very low spatial frequencies are allowed in the EEG inversions, whereas higher spatial frequencies are admitted in both radial and tangential MEG inversions, with the tangential MEG actually allowing slightly more spatial information into the inversion than the radial MEG. Since source resolution is directly related to the degree of regularization, this graph suggests that inversions from the EEG outside the skull will offer lower spatial resolutions than inversions from the MEG.

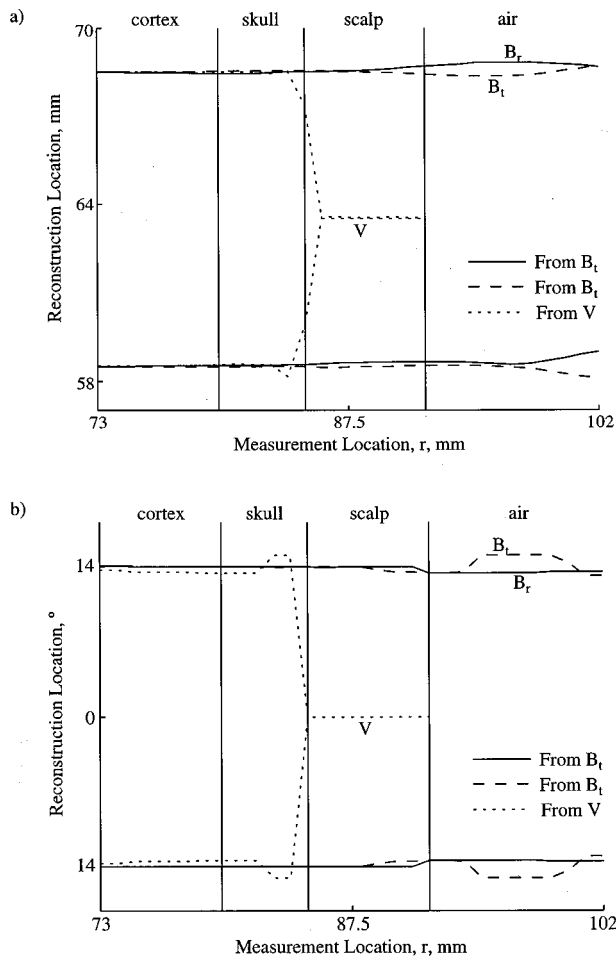


FIGURE 6. Location of each source as a function of measurement location for (a) the aligned sources and (b) the parallel sources. Inversions from EEG calculated outside the skull layer must be regularized to the extent that two sources appear at one location. MEG inversions correctly locate the sources from all measurement positions.

The results presented thus far are due to volume conduction effects and are not directly related to particular source parameters. Thus, similar results to those illustrated in Figs. 4 and 5 for the case of aligned sources are observed with the parallel source configuration. We will now explicitly show the effects of volume conduction on the spatial resolution of both the aligned and parallel sources.

Spatial Resolution Effects

Source Localizing Resolution. Regularization of the inversion implies the loss of spatial information at higher spatial frequencies. If the regularization process filters out information at spatial frequencies that are too low, the spatial resolution of the inversion may not be sufficient to distinguish two sources. Figure 6(a) shows the localizing resolution for the aligned sources while Fig.

6(b) shows localization of the parallel sources. The MEG signals do not require as much regularization as the EEG signals, and so they tend to locate each source accurately at all calculation points throughout the head model. On the other hand, the EEG outside the skull layer must be regularized to such an extent that the two sources are localized to the same position. This effect is seen for both aligned and parallel source configurations. The skull introduces an additional low-pass operation on the EEG signals (in addition to the low-pass operation caused by the decay of the signal with distance from the source), and thereby smooths and attenuates the EEG signals. Again we see that the effect of the skull layer is to reduce the spatial information contained in the EEG so much that regularization of the inversion destroys information about source distinctness.

Source Imaging Resolution. While the location of the reconstructed sources indicates the localizing resolution, the imaging resolution is related to the width of the reconstructed sources. As lower window cutoff frequencies are required, less spatial frequency information is allowed into the inversion, and the reconstruction broadens, becoming less distinct [see Fig. 4(b)]. If two sources are broadened severely, they may be unresolved. The degree to which two sources are resolved is tested by the Rayleigh criterion. Figures 7(a) and 7(b) show the valley-to-peak ratio for source reconstructions from each modality plotted against distance from the source for the aligned and parallel source configurations, respectively. Similar effects are observed for both source configurations. The EEG outside the skull layer does not meet the Rayleigh criterion, and the two sources are considered unresolved. Both radial and tangential magnetic fields are adequately resolved at all calculated locations. This graph implies that large source separations are necessary for the EEG to distinguish sources, whereas the MEG is able to distinguish sources that are separated by much smaller distances. The tangential magnetic fields provide for higher resolution than do the radial magnetic fields, particularly for the parallel source configuration.

The results obtained in this work depend strongly on the model parameters used and the amount and type of noise simulated. We can quantify this with a sensitivity analysis. There are two ways to proceed. We can calculate the effect of varying parameters on forward calculations. This method will let us see directly how a particular model affects the forward fields. An alternative method is to use the forward fields obtained with "typical" model parameters to perform inversions in which model parameters are varied. This method more closely resembles the potentially realistic situation in which a researcher might make incorrect model assumptions for an inverse analysis applied to actual data in which the precise parameters are unknown. Both types of analyses

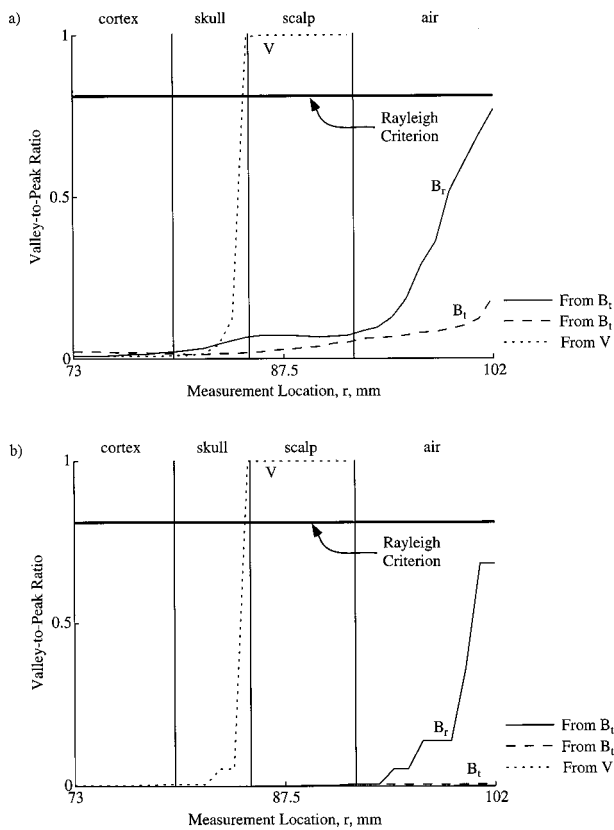


FIGURE 7. Imaging resolution of the two sources defined by the valley-to-peak ratio as a function of measurement location for (a) aligned and (b) parallel source configurations. EEG inverse solutions exceed the Rayleigh criterion and are considered unresolved for calculations outside the skull layer. MEG solutions are resolved for all calculation locations. Tangential MEG exhibits higher imaging resolution than does the radial MEG.

were performed by Bradshaw⁶ and will be summarized here.

Sensitivity to Conductivity and Geometry

The conductivity and geometrical parameters used in the head model affect the spatial filters. We can examine the effects of varying these parameters by determining the changes they cause in the spatial filters. To quantify this, we determine the spatial resolution in terms of the maximum window cutoff frequency for stable reconstructed sources ($\xi \geq 0.96$) while varying conductivity and geometry parameters of the model. Figure 8 shows the effect of varying parameters on inverse regularization for the scalp EEG, and the radial and tangential MEG in air 1 cm from the scalp surface. The conductivities of the brain and scalp are varied from one tenth to ten times their nominal value while the skull conductivity is varied over two ranges; one over one tenth to ten times its typical values and another over the same range as the cortex and scalp conductivities are varied. Figure 8(a)

shows that conductivity parameters affect *only* EEG and have very little effect on either radial or tangential MEG. Low values of cortical and scalp conductivity result in higher achievable spatial resolution for EEG while values greatly above the nominal value of $0.45/\Omega \text{ mm}^{-1}$ actually *decrease* the amount of spatial information in EEG reconstructions. This fact may seem somewhat counterintuitive since one might expect that more conductive tissue would necessarily result in higher spatial resolution. However, it must be noted that the effect of low-conductivity layers is dependent on the *ratio* in conductivity between two layers rather than on the absolute conductivities. Thus, higher values of cortex and scalp conductivity are further away from the skull conductivity, and the spatial resolution decreases. For precisely the same reason, values for skull conductivity that are lower than typical also decrease the spatial resolution, as expected. It is not surprising to note that the maximum spatial resolution obtainable from EEG would occur if the skull conductivity exactly matched that of the cortex and scalp.

Changing the geometrical parameters of the model has similar effects on all three measurement modalities [Fig. 8(b)], although the resolution from radial and tangential MEGs does not decrease as severely as the EEG. The effect on the magnetic signals is primarily a result of the increased source-measurement distance. For the EEG, the distance increase aggravates the effect of conductivity discontinuities. Thus, while the EEG is affected by both geometrical and conductivity factors, effects on the MEGs are largely limited to geometrical considerations. These results are consistent with the study by Hämmäläinen and Sarvas,²² who showed minor MEG differences exist between spherical head models with and without realistic conductivities, but major differences exist between spherical head models and realistic geometry models.

Sensitivity to Noise Level

A measure of the degree to which noise affects the results obtained in this simulation is also desired. The calculations in this work assumed spatially white measurement noise with levels of 20% for the EEG, and 30% for the MEG. We can ascertain how the noise level affects the spatial resolution of reconstructions by calculating the maximum window cutoff frequency allowed for reconstructions with stability greater than 0.96 while varying the level of white noise. Figure 9 shows the inverse resolution in terms of window cutoff frequency as the noise level increases. The maximum window cutoff allowed in inverse reconstructions is smaller with increasing noise levels, as expected. Increased measurement noise levels are particularly a problem for the scalp EEG, while the radial and tangential MEG are not as

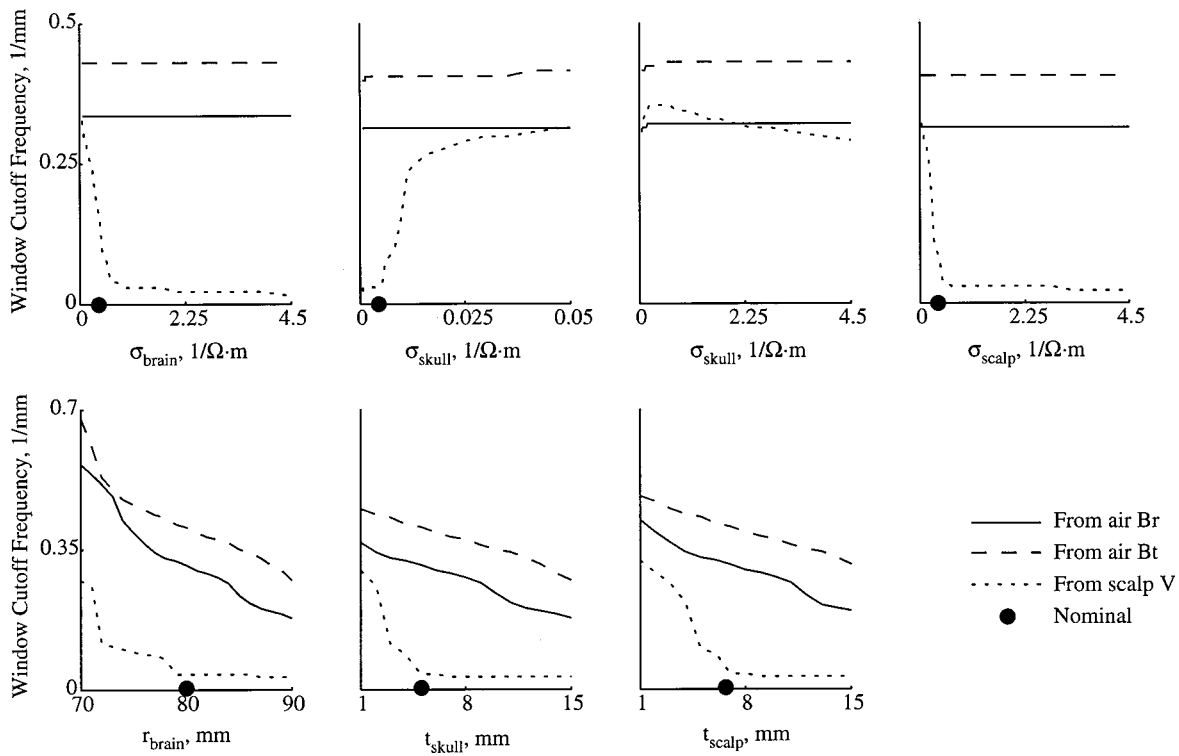


FIGURE 8. Window cutoff frequency, i.e., amount of regularization, required to achieve inverse stability of at least 0.96 as a function of various model parameters. (a) Radial and tangential MEG calculations in air show little response to conductivity variations whereas conductivity changes greatly influence the window cutoff frequency required for EEG inversions. (b) All modalities are affected by geometrical changes.

sensitive to an increased level of measurement noise. Increased noise levels are amplified by the high-pass inverse spatial filters and more regularization is required to achieve stable source reconstructions. As a result, the

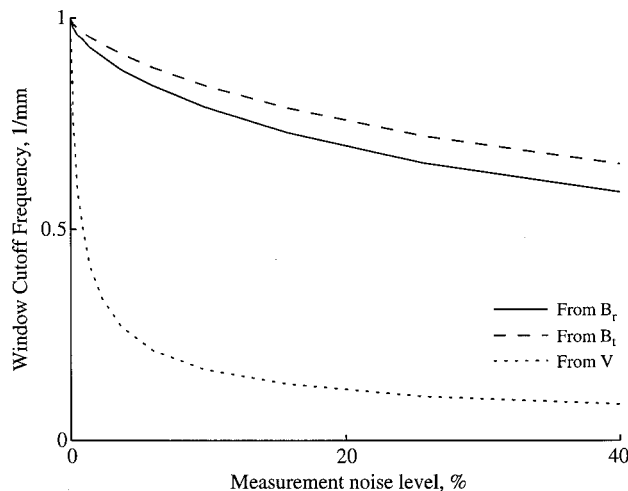


FIGURE 9. Window cutoff frequency required for a reconstruction stability of at least 0.96 as a function of the level of measurement noise. As the additive white-noise level is increased and the signal-to-noise ratio decreases, lower window cutoff frequencies are required to maintain inverse stability.

effect of increasing noise is to limit the spatial resolution in an inverse reconstruction. This calculation suggests that increased measurement noise will not significantly degrade any advantages of MEG over EEG as far as spatial resolution is concerned.

In some cases, measurement noise is not spatially random and uniform, for example, when the “noise” is in fact the spatially correlated background EEG.²⁸ “Brain noise” will also affect the quality of inverse reconstructions if it is amplified by high-pass inverse spatial filters. However, noise from physiological sources is subject to the same low-pass spatial filtering of the volume conducting head as the EEG and MEG signals. Figure 10 shows the effects of independently increasing both brain noise and measurement noise on the window cutoff frequency required for stable ($\xi \geq 0.96$) inversion. If no measurement noise is present, the spatial resolution from the EEG and both radial and tangential MEGs have an identical response to increasing brain noise, since it is low-pass filtered by the layers of the head model in the same manner for all modalities. However, if any measurement noise is present, a dramatic decrease in resolution from the EEG is apparent with increasing brain noise. The low-pass filtered brain noise simply adds to the measurement noise and reduces the amount of spatial

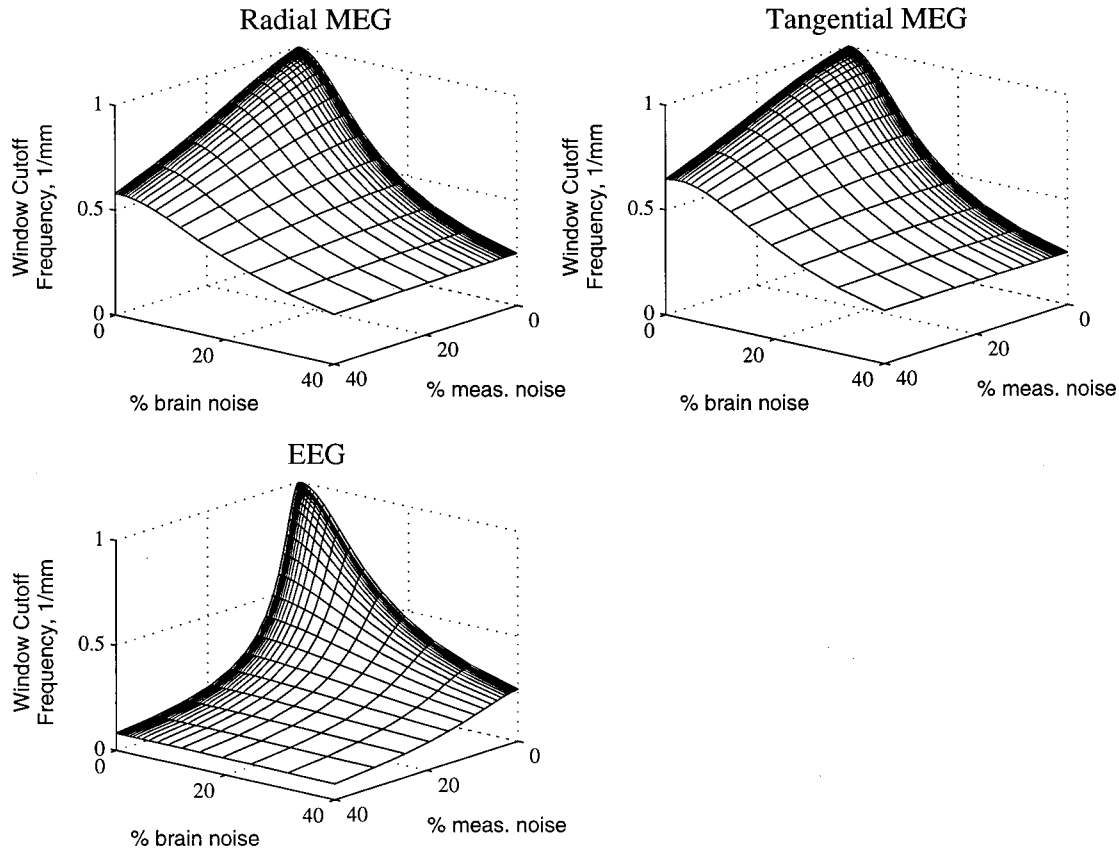


FIGURE 10. Window cutoff frequency required for a reconstruction stability of at least 0.96 as a function of increasing brain noise from 0% to 40% of the maximum source current density and measurement noise from 0% to 40% of the EEG or MEG signal amplitude. All modalities have identical response to brain noise when no measurement noise is present, but in the presence of measurement noise, the EEG resolution is worse than that of comparable noise levels in the MEG.

frequency information available to a stable inverse reconstruction. Once again, this effect is more pronounced for the EEG than for the radial or tangential MEG.

DISCUSSION

The spatial filtering construct allows us to directly visualize several important effects present in the estimation of cortical current sources from external magnetic fields and potentials. The external fields are smoothed and attenuated representations of the internal current density. The most noticeable effect is that of the measurement distance from the source. Measurements taken from greater distances have smaller amplitudes and contain less spatial information. The presence of the low-conductivity skull layer additionally decreases the signal amplitude and spatial information contained in the EEG signals, but has little effect on the magnetic fields. Once the effect of the skull on the potential is realized, very little signal loss occurs in the EEG throughout the scalp layer. The MEG amplitude, on the other hand, continues

to fall off as measurement distance is increased. Recently, Kuc noted that reducing the separation between the magnetometer and the source resulted in a higher signal-to-noise ratio than reducing the noise level by the same factor.²⁶ This result is consistent with the findings of an earlier spatial filtering analysis.⁴² The calculations in this work suggest that significant advantages over EEG are only realized if the measurement distance is kept sufficiently small. The scalp-magnetometer separation needed to provide imaging resolution (of two sources separated by 1 cm) equal to scalp EEG is shown in Fig. 11 for both radial and tangential MEG as a function of source depth below the skull. The radial MEG provides the same resolution as scalp EEG for the detector located roughly 1 cm from the surface of the scalp as long as the sources are not deeper than about 2.5 cm in the cortex. For source depths beyond 2.5 cm, the radial MEG sensor must be placed progressively closer to the scalp to achieve the same resolution as scalp EEG. The tangential MEG provides resolution equal to scalp EEG with scalp-detector distances of 3 cm, and exhibits

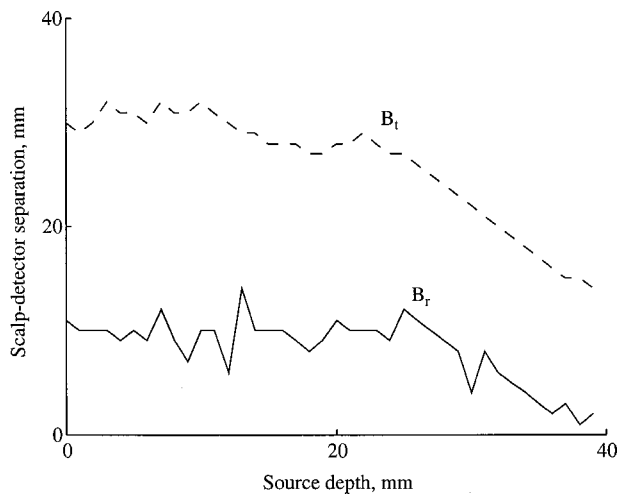


FIGURE 11. Detector distance from the scalp at which the resolution from radial and tangential MEG source reconstructions is equivalent to scalp EEG source reconstructions is plotted as a function of source depth in the cortex. For these model parameters, and two sources separated by 1 cm, radial MEG provides the same resolution as scalp EEG at detector distances of roughly 1 cm unless the source is deeper than 2.5 cm in the cortex. For source depths below 2.5 cm, the radial MEG must be measured progressively closer to the scalp to achieve the same resolution as the EEG. The tangential MEG behaves similarly, but larger detector distances are allowed since the signal amplitude is larger.

a similar degradation in resolution with source depths beyond 2.5 cm below the cortical surface.

Previous work indicates that intervening layers with conductivity discontinuities should not affect the external radial MEG outside an axially symmetric volume conductor,^{20,45} but some effect might be seen in tangential MEG signals. In this study, neither the radial nor tangential MEG reflected any significant contribution from model layers owing primarily to the high degree of symmetry afforded by the cylindrical model. Presumably, the results could differ significantly in realistic head geometries where volume conduction effects might be more pronounced on external magnetic fields, although the work of Hämäläinen and colleagues suggests otherwise.²² Also, our model is restricted to the consideration of sources tangential to the surface of the head, and deviations from tangential orientation of sources would be expected to degrade the MEG performance,³⁸ although we note that cortical sources detected by MEG or EEG are largely believed to be tangential in orientation.⁵⁵ These questions may be addressed in future work.

Our work shows that the tangential field amplitudes are as much as four times greater than the radial field amplitudes, and thus, the SNR of the tangential MEG may be higher than that of the radial MEG. The tangential MEG therefore contains more spatial information

than does the radial MEG at a given measurement location. Tangential magnetic fields have been recorded in the study of magnetocardiogram (MCG),^{3,25,35,41} but their general usefulness and relation to the radial magnetic fields have not been demonstrated. One important advantage of tangential recordings over radial measurements in dipole localization is the fact that tangential magnetic fields have peaks directly above the dipoles, whereas peaks in the radial signal are laterally displaced from the actual dipole location. The results did not differ when the separation of the two sources was not along their electric orientation. The parallel source configuration is subject to the same spatial filtering as are the aligned sources. Thus, the only noted effect of changing the orientation of the separation was to improve the imaging resolution of the tangential MEG (Fig. 7).

Framing the forward and inverse problems of MEG and EEG in terms of spatial filters also clarifies the difference between localizing and imaging resolution. Consider a one-dimensional example with a single 1-mm-wide current source located along the x axis at $x = 0$ mm that extends from $x = -0.5$ mm to $x = +0.5$ mm. If the measurement domain is sufficiently large (say, $x = -10$ mm to $x = +10$ mm), the spatial information about the source's location in the measurement domain is contained primarily at a spatial frequency that corresponds to the distance between the edge of the measurement and the location of the source, or $f_{loc} = 1/10 \text{ mm}^{-1}$ in our example. The spatial extent of the source, or the image of the source, is associated primarily with a spatial frequency of $f_{image} = 1/1 \text{ mm}^{-1}$. Thus, the imaging resolution is determined by the amount of information contained at higher spatial frequencies than the localizing resolution. Since the intervening layers between the source and the measurement are effectively low-pass filters, they will tend to filter out the higher spatial frequencies, and thus, typically, imaging resolution is lower than localizing resolution. If more than one source is present, reduction in the imaging resolution by regularization will "blur" the sources, as we have shown in this work. Eventually, regularization can reduce the imaging resolution to such an extent that the sources are blurred together and appear as one source.

Inverse reconstructions from the MEG were better resolved than were reconstructions from the EEG, with tangential MEG reconstructions the most accurate. Table 2 shows 3 dB points for the low-pass forward filters (which are also 3 dB points for the high-pass inverse filters). Since the forward filters for the MEG do not fall off at spatial frequencies as low as with the EEG, the MEG inverse filters require less regularization at low spatial frequencies and are able to retain more spatial information. This type of spatial filtering analysis could be applied to other bioelectric phenomena where volume conduction is important, as is the case with gastrointes-

TABLE 2. 3 dB roll-off points for EEG and MEG forward and inverse filters [(mV or pT)/(μ A/mm²)].

Signal	3 dB point
MEG, radial	0.0625
MEG, tangential	0.0703
EEG	0.0234

tinal activity. Low-conductivity layers between gastrointestinal sources and the abdominal wall severely attenuate cutaneous potentials, but leave magnetic fields relatively unaffected.⁸

This analysis simulated magnetic field detectors whereas most common biomagnetometer systems actually measure field gradients. Likewise, the potential calculations in this work are referred to a distant point where the potential is zero. In actual practice, the reference electrode is a major concern in EEG measurement as is the choice of a particular gradiometric arrangement for proper elimination of signal artifacts.¹⁶ Though we do not attempt to address these specific problems in this work, we deal with the issue of the surface Laplacian, which is effectively a second spatial derivative of the EEG or MEG signals, in the companion paper.⁷

Our sensitivity analysis showed that varying geometrical parameters affected both the EEG and the MEG whereas varying conductivity parameters affected only the EEG. Also, increased noise level (or, equivalently, decreased SNR) significantly affects the ability of the inverse procedure to provide accurate reconstructions. Random noise appears to affect the EEG more than the MEG since it is amplified by the high-pass inverse filters and must be regularized, thus reducing the spatial resolution. Background brain noise that is spatially correlated can also dramatically decrease the maximum achievable spatial resolution in inverse reconstructions, particularly when measurement noise is also present.

Although this analysis suggests that under the conditions specified, the spatial resolution of the MEG is theoretically superior to that of the EEG for superficial tangential cortical current sources and state-of-the-art magnetometers, several authors have suggested that advanced signal processing techniques such as the surface Laplacian operation may significantly improve the EEG spatial resolution.^{2,30,36} We present a similar comparison of the MEG and EEG surface Laplacians in the accompanying paper.⁷

ACKNOWLEDGMENTS

This work was supported in part by a University Graduate Fellowship from the Graduate School at Vanderbilt University and by National Institutes of Health Grant No. 1 R43 DK-49435-01.

REFERENCES

- Arthur, R. M. and D. B. Geselowitz. Effect of inhomogeneities on the apparent location and magnitude of a cardiac current dipole source. *IEEE Trans. Biomed. Eng.* 17:141–146, 1970.
- Babiloni, F., C. Babiloni, L. Fattorini, F. Carducci, P. Onorati, and A. Urbano. Performances of surface Laplacian estimators: A study of simulated and real scalp potential distributions. *Brain Topogr.* 8:35–45, 1995.
- Barry, W. H., W. H. Fairbank, D. C. Harrison, K. L. Lehrman, J. A. V. Malmivuo, and J. P. Wikswo, Jr. Measurement of the human magnetic heart vector. *Science* 198:1159–1162, 1977.
- Baumgartner, C. MEG, EEG, and ECoG: Discussion. *Acta Neurol. Scand. Suppl.* 152:91–92, 1994.
- Born, M., and E. Wolf. *Principles of Optics*. New York: Pergamon, 1975.
- Bradshaw, L. A. Measurement and Modeling of Gastrointestinal Bioelectric and Biomagnetic Fields. PhD Dissertation, Vanderbilt University, 1995.
- Bradshaw, L. A., and J. P. Wikswo, Jr. A spatial filter approach for evaluation of the surface Laplacian of EEG and MEG. *Ann. Biomed. Eng.* 29:202–213, 2001.
- Bradshaw, L. A., S. H. Allos, J. P. Wikswo, Jr., and W. O. Richards. Correlation and comparison of magnetic and electric detection of small intestinal electrical activity. *Am. J. Physiol.* 272:G1159–G1167, 1997.
- Brenner, D., J. Lipton, L. Kaufman, and S. J. Williamson. Somatically evoked magnetic fields of the human brain. *Science* 199:81–83, 1978.
- Clark, J. and R. Plonsey. The extracellular potential field of the single active nerve fiber in a volume conductor. *Biophys. J.* 8:842–864, 1968.
- Cohen, D., B. N. Cuffin, K. Yunokuchi, R. Maniewski, C. Purcell, G. R. Cosgrove, J. Ives, and J. G. Kennedy. MEG versus EEG localization test using implanted sources in the human brain. *Ann. Neurol.* 28:811–817, 1990.
- Cohen, D. and B. N. Cuffin. Demonstration of useful differences between magnetoencephalogram and electroencephalogram. *Electroencephalogr. Clin. Neurophysiol.* 56:38–51, 1983.
- Cuffin, B. N. and D. Cohen. Comparison of the magnetoencephalogram and electroencephalogram. *Electroencephalogr. Clin. Neurophysiol.* 47:132–146, 1979.
- Dallas, W. J. Fourier space solution to the magnetostatic imaging problem. *Appl. Opt.* 24:4543–4546, 1985.
- Ganapathy, N., and J. W. Clark. Extracellular potentials from skeletal muscle. *Math. Biosci.* 83:61–96, 1987.
- Gencer, N. G., S. J. Williamson, A. Gueziec, and R. Hummel. Optimal reference electrode selection for electric source imaging. *Electroencephalogr. Clin. Neurophysiol.* 99:163–173, 1996.
- Geselowitz, D. B. On bioelectric potentials in an inhomogeneous volume conductor. *Biophys. J.* 7:1–11, 1967.
- Geselowitz, D. B. On the magnetic field generated outside an inhomogeneous volume conductor by internal current sources. *IEEE Trans. Magn.* 6:346–347, 1970.
- Gielen, F. L. H., B. J. Roth, and J. P. Wikswo, Jr. Capabilities of a toroid-amplifier system for magnetic measurement of current in biological tissue. *IEEE Trans. Biomed. Eng.* 33:910–921, 1986.
- Hämäläinen, M. S., R. Hari, R. J. Ilmoniemi, J. Knuutila, and O. V. Lounasmaa. Magnetoencephalography—Theory, instrumentation, and applications to noninvasive studies of the

- working human brain. *Rev. Mod. Phys.* 65:413–497, 1993.
- ²¹Hämäläinen, M. S., and R. J. Ilmoniemi. Interpreting measured magnetic fields of the brain: Estimates of current distributions. (Helsinki University of Technology, Finland), Technical Report No. TKK-F-A559, 1984.
- ²²Hämäläinen, M. S. and J. Sarvas. Realistic conductivity geometry model of the human head for interpretation of neuromagnetic data. *IEEE Trans. Biomed. Eng.* 36:165–171, 1989.
- ²³Hari, R., M. Hämäläinen, R. Ilmoniemi, and O. V. Lounasmaa. MEG versus EEG localization test. Letter to the Editor. *Ann. Neurol.* 30:222–223, 1991.
- ²⁴Jackson, J. D. *Classical Electrodynamics*. New York: Wiley, 1975.
- ²⁵Kandori, A., K. Tsukada, T. Haruta, Y. Noda, Y. Terada, T. Mitsui, and K. Sekihara. Reconstruction of two-dimensional current distribution from tangential MCG measurement. *Phys. Med. Biol.* 41:1705–1716, 1996.
- ²⁶Kuc, R. Magnetometer spacing criterion for biomagnetic source imaging. *IEEE Trans. Biomed. Eng.* 43:1125–1127, 1996.
- ²⁷Kullmann, W. and W. J. Dallas. Fourier imaging of electrical currents in the human brain from their magnetic fields. *IEEE Trans. Biomed. Eng.* 34:837–842, 1987.
- ²⁸Law, S. K., P. L. Nunez, and R. S. Wijesinghe. High-resolution EEG using spline generated surface Laplacians on spherical and ellipsoidal surfaces. *IEEE Trans. Biomed. Eng.* 40:145–153, 1993.
- ²⁹Le, J., and A. Gevins. Method to reduce blur distortion from EEGs using a realistic head model. *IEEE Trans. Biomed. Eng.* 40:517–527, 1993.
- ³⁰Le, J., V. Menon, and A. S. Gevins. Local estimate of surface Laplacian derivation on a realistically shaped scalp surface and its performance on noisy data. *Electroencephalogr. Clin. Neurophysiol.* 92:433–441, 1994.
- ³¹Lutkenhoner, B. A simulation study of the resolving power of the biomagnetic inverse problem. *Clin. Phys. Physiol. Meas.* 12:73–78, 1991.
- ³²Malmivuo, J., V. Suihko, and H. Eskola. Sensitivity distributions of EEG and MEG measurements. *IEEE Trans. Biomed. Eng.* 44:196–208, 1997.
- ³³Mosher, J. C., M. E. Spencer, R. M. Leahy, and P. S. Lewis. Error bounds for EEG and MEG dipole source localization. *Electroencephalogr. Clin. Neurophysiol.* 86:303–321, 1993.
- ³⁴Murro, A. M., J. R. Smith, D. W. King, and Y. D. Park. Precision of dipole localization in a spherical volume conductor: A comparison of referential EEG, magnetoencephalography, and scalp current density methods. *Brain Topogr.* 8:119–125, 1995.
- ³⁵Nousiainen, J., O. S. Oja, and J. Malmivuo. Normal vector magnetocardiogram. I. Correlation with the normal vector ECG. *J. Electrocardiol.* 27:221–231, 1994.
- ³⁶Nunez, P. L., and K. L. Pilgreen. The spline Laplacian in clinical neurophysiology: A method to improve EEG spatial resolution. *J. Clin. Neurophysiol.* 8:397–413, 1991.
- ³⁷Okada, Y. C. Neurogenesis of evoked magnetic fields. In: *Biomagnetism: An Interdisciplinary Approach*, edited by S. J. Williamson, G.-L. Romani, L. Kaufman, and I. Modena. New York: Plenum, 1982, pp. 399–408.
- ³⁸Pascual-Marqui, R. D., and R. Biscay-Lirio. Spatial resolution of neuronal generators based on EEG and MEG measurements. *Int. J. Neurosci.* 68:93–105, 1993.
- ³⁹Proakis, J. G., and D. G. Manolakis. *Introduction to Digital Signal Processing*. New York: Macmillan, 1988.
- ⁴⁰Rall, W. Branching dendritic trees and motoneuron membrane resistivity. *Exp. Neurol.* 1:491–527, 1959.
- ⁴¹Rosen, A. and G. T. Inouye. A study of the vector magnetocardiographic wave form. *IEEE Trans. Biomed. Eng.* 22:167–174, 1975.
- ⁴²Roth, B. J., N. G. Sepulveda, and J. P. Wiksw, Jr. Using a magnetometer to image a two-dimensional current distribution. *J. Appl. Phys.* 65:361–372, 1989.
- ⁴³Roth, B. J., and J. P. Wiksw, Jr. The electrical potential and the magnetic field of an axon in a nerve bundle. *Math. Biosci.* 76:37–57, 1985.
- ⁴⁴Rush, S., and D. A. Driscoll. EEG electrode sensitivity—An application of reciprocity. *IEEE Trans. Biomed. Eng.* 16:15–22, 1969.
- ⁴⁵Sarvas, J. Basic mathematical and electromagnetic concepts of the biomagnetic inverse problem. *Phys. Med. Biol.* 32:11–22, 1987.
- ⁴⁶Singh, M., R. R. Brechner, and V. W. Henderson. Neuro-magnetic localization using magnetic resonance images. *IEEE Trans. Biomed. Eng.* 11:129–134, 1992.
- ⁴⁷Srinivasan, R., P. L. Nunez, and R. B. Silberstein. Spatial filtering and neocortical dynamics: Estimates of EEG coherence. *IEEE Trans. Biomed. Eng.* 45:814–826, 1998.
- ⁴⁸Stampfli, R. In: *Demyelinating Disease, Basic Clinical Electrophysiology*, edited by S. G. Waxman and J. M. Ritchie. New York: Raven, 1981.
- ⁴⁹Tan, S., B. J. Roth, and J. P. Wiksw, Jr. The magnetic field of cortical current sources: The application of a spatial filtering model to the forward and inverse problems. *Electroencephalogr. Clin. Neurophysiol.* 76:73–85, 1990.
- ⁵⁰Wijesinghe, R. S. A mathematical model for calculating the vector magnetic field of a single muscle fiber. *Math. Biosci.* 103:245–274, 1991.
- ⁵¹Wiksw, Jr. J. P., High-resolution magnetic imaging: Cellular action currents and other applications. In: *NATO ASI on SQUID Sensors: Fundamentals, Fabrication and Applications*, edited by H. Weinstock. Dordrecht: Kluwer (in press).
- ⁵²Wiksw, Jr., J. P., A. S. Gevins, and S. J. Williamson. The future of the EEG and MEG. *Electroencephalogr. Clin. Neurophysiol.* 87:1–9, 1993.
- ⁵³Wiksw, Jr., J. P., and B. J. Roth. Magnetic determination of the spatial extent of a single cortical current source: A theoretical analysis. *Electroencephalogr. Clin. Neurophysiol.* 69:266–276, 1988.
- ⁵⁴Williamson, S. J. MEG versus EEG localization test. Letter to the Editor. *Ann. Neurol.* 30:222, 1991.
- ⁵⁵Wood, C. C., D. Cohen, B. N. Cuffin, M. Yarita, and T. Allison. Electrical sources in human somatosensory cortex: Identification by combined magnetic and and potential recordings. *Science* 227:1051–1053, 1985.
- ⁵⁶Woolsey, J. K., B. J. Roth, and J. P. Wiksw, Jr. The magnetic field of a single axon: A volume conductor model. *Math. Biosci.* 76:1–36, 1985.